Three dimensional photoacoustic imaging of vascular anatomy in small animals using an optical detection system

Edward Z. Zhang*, Jan Laufer and Paul Beard
Department of Medical Physics and Bioengineering, University College London
Malet Place Engineering Building, Gower Street, London WC1E 6BT, UK
Website: http://www.medphys.ucl.ac.uk/research/mle/index.htm

ABSTRACT

A 3D photoacoustic imaging instrument for characterising small animal models of human disease processes has been developed. The system comprises an OPO excitation source and a backward-mode planar ultrasound imaging head based upon a Fabry Perot polymer film sensing interferometer (FPI). The mirrors of the latter are transparent between 590 – 1200nm but highly reflective between 1500-1600nm. This enables nanosecond excitation laser pulses in the former wavelength range, where biological tissues are relatively transparent, to be transmitted through the sensor head into the tissue. The resulting photoacoustic signals arrive at the sensor where they modulate the optical thickness of the FPI and therefore its reflectivity. By scanning a CW focused interrogating laser beam at 1550nm across the surface of the sensor, the spatial-temporal distribution of the photoacoustic signals can therefore be mapped in 2D enabling a 3D photoacoustic image to be reconstructed. To demonstrate the application of the system to imaging small animals such as mice, 3D images of the vascular anatomy of the mouse brain and the microvasculature in the skin around the abdomen were obtained non invasively. It is considered that this system provides a practical alternative to photoacoustic scanners based upon piezoelectric detectors for high resolution non invasive small animal imaging.

Keywords: Photoacoustic, ultrasound array, biomedical, small animal imaging, Fabry Perot sensor, 3D imaging

1. INTRODUCTION

Photoacoustic imaging is an effective non-invasive tool for imaging soft tissue, of which the high optical scattering and low acoustic contrast would otherwise render either poor spatial resolution or lack of image contrast if optical imaging or ultrasound is used alone. The technique relies upon generating acoustic energy inside a volume of soft tissue by illuminating it with pulsed visible or near infrared (NIR) laser light. The thermoelastic expansion produces broadband (tens of MHz) pulses of acoustic energy, which propagate to the surface where they are detected by an array of ultrasound receivers. By measuring the time of arrival of the acoustic pulses at each element of the array, and with knowledge of the speed of sound in tissue, the acoustic signals can be spatially resolved and back-projected to form an image of the internally distributed photoacoustic sources. By encoding the spatial distribution of tissue optical properties on to broadband ultrasound waves in this way, the technique combines the advantages of the strong contrast and spectroscopic capability offered by optical methods with the high spatial resolution available to ultrasound. The high optical contrast within the soft tissue is mainly due to the high optical absorption of haemoglobin in the visible and NIR. The latter has a strong spectroscopic correlation with the oxygenation state. Thus, the photoacoustic technique is particularly useful for structural and functional imaging of vasculature and a variety of applications have been explored ranging from imaging the breast for the diagnosis and screening of cancer [1, 2], the assessment of vascular disease, structural and functional imaging of the rat brain [3] and imaging the microvasculature [4, 5, 6, 7].

For short range high resolution applications, such as imaging the skin where it is required to visualise microvessels which lie within a few mm of the surface, it is highly desirable to be able to detect the photoacoustic signals over the same region of the tissue surface that is irradiated: the so-called backward mode of operation. In this paper we report a 2D photoacoustic imaging system based on a Fabry-Perot (FP) polymer film ultrasound sensor [8,9,10,11,12] that can achieve this. In contrast to a previously described FP sensor, which was designed to be transparent to excitation laser

* ezzhang@medphys.ucl.ac.uk; phone +44 20 7679 0281.

Photons Plus Ultrasound: Imaging and Sensing 2007: The Eighth Conference on Biomedical Thermoacoustic, Optoacoustics, and Acousto-optics, edited by Alexander A. Oraevsky, Lihong V. Wang,
Proc. of SPIE Vol. 6437, 64370S, (2007) · 1605-7422/07/$18 · doi: 10.1117/12.700128

pulses at 1064nm [13], the sensor is transparent in the wavelength range 590nm-1200nm and thus coincides with the so-called NIR window of transparency for biological tissues. This enables the system to operate in backward mode with a tunable Optical Parametric Oscillator (OPO) as the excitation source for near infrared (NIR) spectroscopic applications such as the measurement of blood oxygenation [14,15]. The experimental setup of the imaging system is described in Section 2, followed by the evaluation of its performance in Section 3 using tissue mimicking phantoms. Images of the mouse brain and skin microvasculature are presented in Section 4.

2. EXPERIMENTAL SETUP

A schematic of the 3D photoacoustic imaging system is depicted in Figure 1(a). The excitation source is an optical fiber coupled tunable optical parametric oscillator (OPO) laser (590–1200nm). The sensor for mapping the photoacoustic signal is a Fabry-Perot (FP) ultrasound sensor, as shown in Figure 1(b). It has lateral dimensions of 25mm×40mm. The sensing structure is a polymer film interferometer which consists of a Parylene film with dielectric coatings at its two facets, and is vacuum deposited on to a polymer substrate [10], as illustrated in Figure 1(c). The thickness of the film is either of 20µm or 40µm, giving rise to a -3dB acoustic bandwidth of ~40 or ~23 MHz respectively. The dielectric coatings have a dichroic design, which has high reflectivity (>90%) between 1500nm and 1600nm, while the excitation laser pulse in NIR region 590-1200nm can pass through it (>80% transmission) [16]. Such a design enables the imaging system to operate in backward mode.

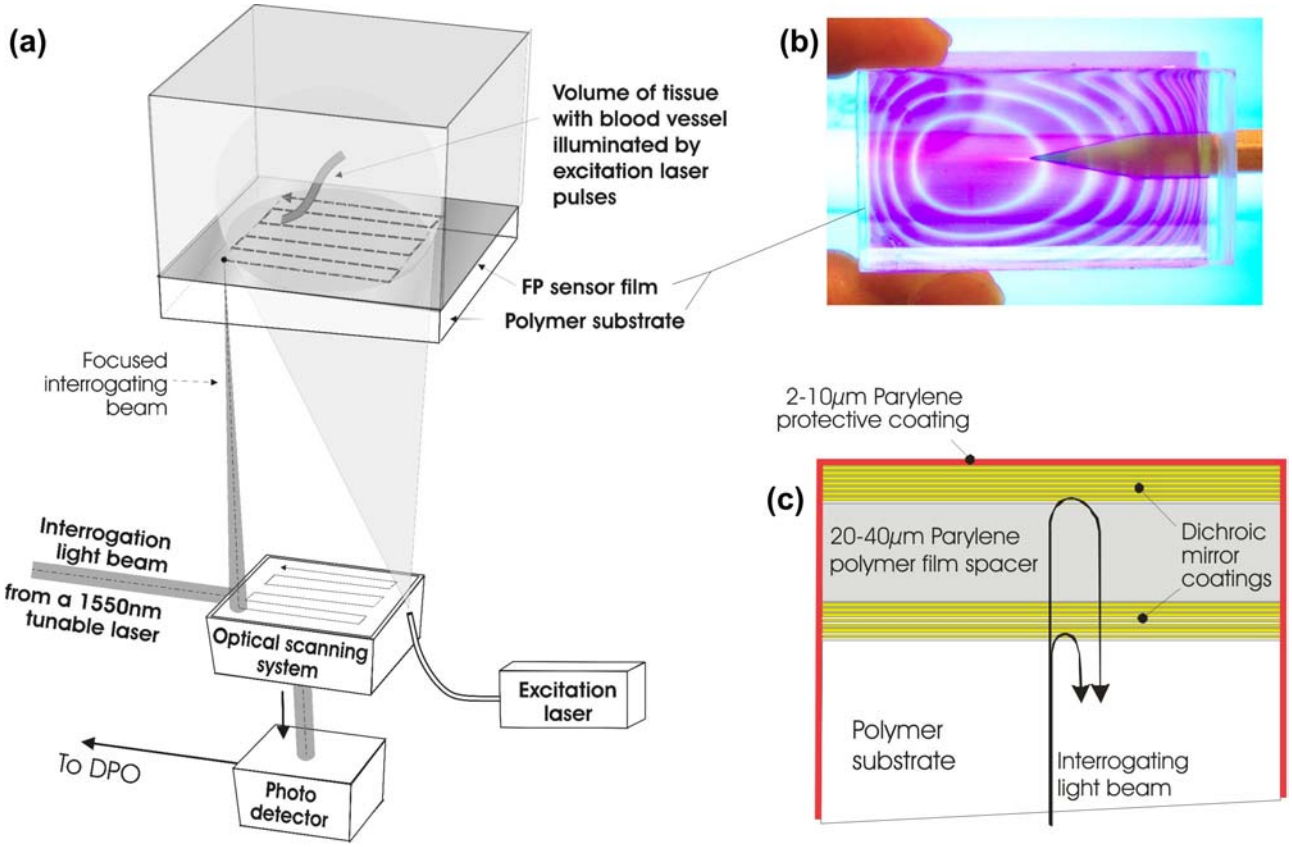

Figure 1: (a) Schematic of the backward mode photoacoustic imaging system; (b) photograph of the FP sensor; (c) configuration of the FP sensor.

The FP sensor is interrogated by a single mode wavelength tunable laser with a tuning range of 1519–1630nm, optical output power output of approximately 10mW, spectral line width (FWHM) <150 kHz and relative intensity noise (RIN)

<140dB/Hz. The incident acoustic wave modulates the optical thickness of FP sensor film which results in a change in the reflected interrogation light. The latter is detected by an InGaAs photodiode (PD). The FP sensor is acoustically non-resonant and in principle provides a broadband response from DC to its upper cut-off frequency. In this system, in order to provide sufficient dynamic range and remove low frequency fluctuations in the interrogation laser output, the detected signal is AC coupled with a low cut-off frequency of 100 kHz.

The FP sensor functions like a planar ultrasound receiver array. The spot size of the interrogating light focused at the FP sensor film is ~38µm diameter (FWHM) which, to a first approximation, represents the active area of a sensing element [17]. The position of each sensing element and the element spacing can be flexibly arranged or rapidly rearranged by controlling how the focused interrogation beam is scanned over the FP sensor with the optical scanning system shown in Figure 1(a). In this work, the array elements are aligned over a linear grid with evenly distributed element spacing along *x* and *y* axis. The arrowed dashed line in Figure 1(a) illustrates an example of the trajectory of the focused spot of interrogation light scanning over the sensor film. The scanning system is galvanometer-based and is also arranged to guide the reflected interrogating light from the FP sensor to the PD.

Before performing a measurement at a specific sensing point or element on the sensor, the wavelength of the interrogation light is tuned in such a way that its reflection from the FP sensing element is most sensitive to the acoustically induced optical phase shift. In other words, at each point, the FP sensor system needs to be optimally phase-biased before a measurement can take place [10].

The operation of the imaging system is controlled by a personal computer (PC) and synchronized with the excitation pulses. During the PA signal mapping process, each point on the sensor is addressed step-by-step by the focused interrogation beam. When the system is ready to accept a photoacoustic signal at a specific point, the digital phosphor oscilloscope (DPO), a Tektronix TDS5000B model operating in FastFrame mode, is armed, allowing it to be triggered by an excitation laser pulse and then capture the photoacoustic waveform. This process is repeated until all the sensing elements have been addressed. At this point the waveforms captured by the DPO are downloaded to the PC. From the photoacoustic signals recorded over the surface of the sensor, a 3D image is reconstructed using a k-space reconstruction algorithm [18].

3. SYSTEM EVALUATION AND PHANTOM STUDIES

The point spread function (PSF) of the imaging system has been evaluated in previous work using a phantom comprising 6 layers of parallel black polymer ribbons [16]. It shows that in addition to its dependence on the bandwidth and active size of the sensing element, the PSF varies with depth and lateral distance from the centre of the scan aperture. Typical values of the PSF at the aperture center and for depths up to 2 mm are 27 µm vertical and 37 µm lateral, for an FP sensor with a sensing film thickness of 20 µm which provides a -3dB acoustic bandwidth of ~40 MHz.

In order to determine the maximum achievable mapping speed of the system, the output of a 20 MHz, planar piezoelectric transducer was mapped over an area of 6 mm × 6 mm as shown in Figure 2(a). The transducer is placed with its output facet parallel to and 0.9 mm away the FP sensor. Figure 2(b) illustrates part of the temporal sequence of the acoustic field images recorded during the mapping process. The time interval between successive frames is 4 ns. The repetition rate of the transducer output is ~6 kHz. The total number of sensing elements is 120 × 120 with 50 µm element spacing. The total mapping time was ~130 seconds, representing a mapping speed of 110 elements per second. However, the mapping speed obtainable from the system will be limited by the repetition rate of the excitation pulse source used. When using the OPO laser which has a pulse repetition rate of 10 Hz, the actual mapping speed is ~10 elements per second.

The acoustic sensitivity of the system is approximately 0.3kPa NEP over a measurement bandwidth of 20MHz and without signal averaging. To evaluate the system for photoacoustic imaging, the two phantoms shown in Figure 3 were imaged. Their 3D images were reconstructed from photoacoustic signal data acquired over ~10000 spatial points without signal averaging. For the phantom shown in Figure 3(a), the excitation source was a 20 Hz, 1064nm Nd:YAG Q switched pulse laser. For the phantom shown in Figure 3(b), the excitation was provided by the 10 Hz OPO laser with

an output wavelength of 800nm. These studies suggest that the imaging system will be able to resolve superficial blood vessels down to a depth of 5-6 mm

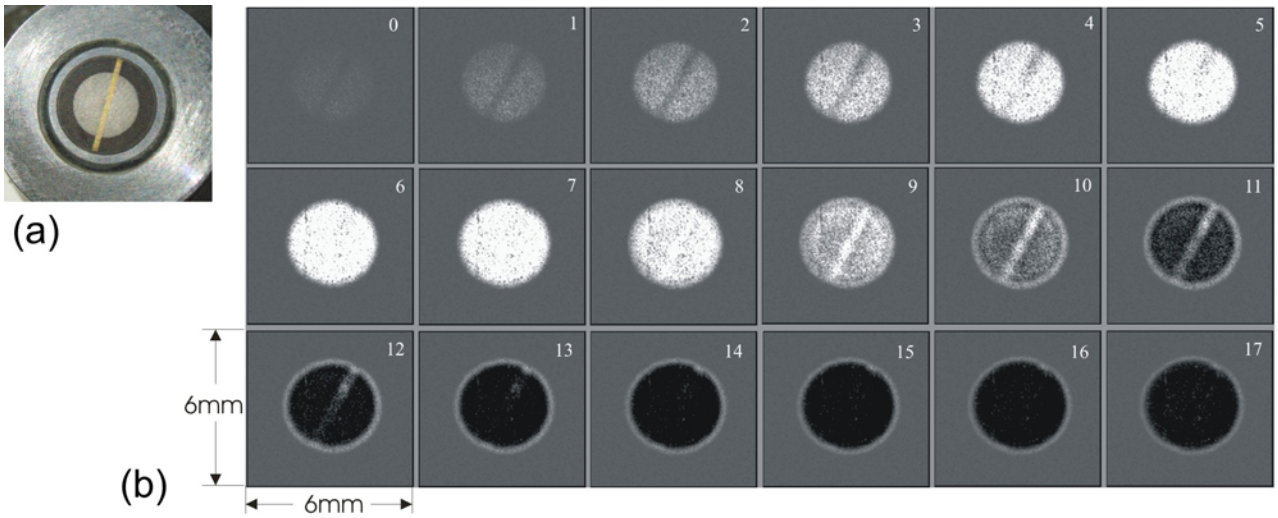

Figure 2: (a) Photograph of the facet of the 20 MHz transducer, the output of which was mapped with the system depicted in Figure 1. (b) Temporal sequence of the recorded acoustic field distribution. The time interval between successive frames is 4ns. The FP sensor was 0.9 mm away from the transducer. The number of sensing elements is 120 × 120, and element spacing is 50 µm.

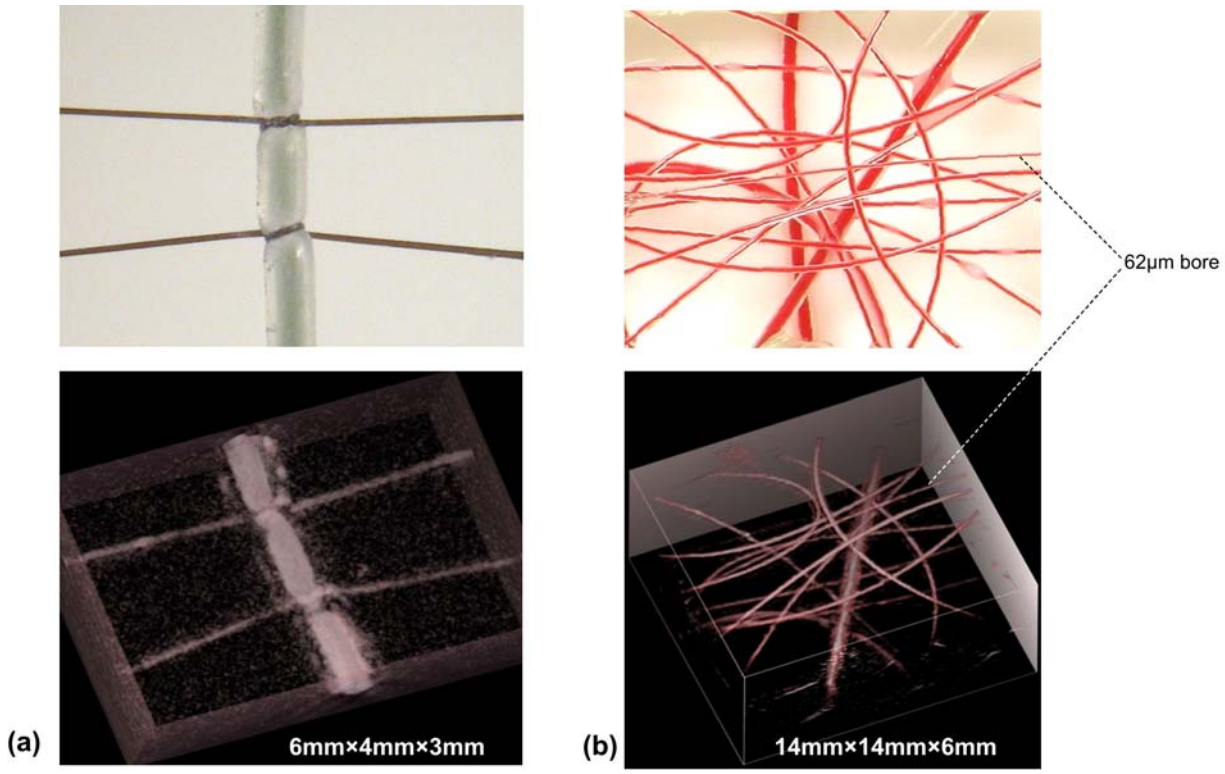

Figure 3: (a) Phantom consisting of 300µm bore silicone rubber tube filled with NIR dye (μ_a=2.7 mm^{-1}) tied with human hair immersed to a depth of ~2 mm in a solution of 1.5% Intralipid (μ_s'=1mm^{-1}), and its 3D photoacoustic image (image volume: 6 mm × 4 mm × 3mm). Excitation wavelength: 1064nm; repetition rate: 20Hz; Incident fluence: 15mJ/cm^2. (b) Phantom submerged in 1.5%

Intralipid (μ_s'=1mm^{-1}) and consisting of polymer tubes filled with human blood (15.2g/dL), and its 3D PA image (14mm × 14mm × 6mm). One tube (as indicated) has a 62µm bore tube and was located at depth between z= 0.9mm and 1.1mm. The rest were 100 µm and 300 µm bore tubes. Most of the 100µm bore tubes were at z=1.1 – 3.5 mm. Two 300µm and a few 100µm bore tubes were at z=3.5 – 5.5 mm. Excitation source: 10 Hz OPO pulsed laser at 800nm. Incident fluence: 6.7mJ/cm^2. Animated version of the volume rendered photoacoustic images can be viewed at: http://www.medphys.ucl.ac.uk/research/mle/images.htm

4. SMALL ANIMAL IMAGING

Ex-vivo small animal imaging experiments were carried out on brown mice. The hair around the parts of body to be imaged was removed using VEET™ hair removal cream. The object-sensor coupling medium was saline. The excitation source was the 10 Hz OPO laser with pulse duration of 8 ns and the incident fluence was less than 10 mJ/cm^2. As with the phantom studies in the previous section, no signal averaging was used.

4.1. 3D imaging of vascular anatomy in mouse brain

The imaging was carried out over the area indicated by the dashed line in Figure 4(a), with the skull intact. The signal (637nm) and idler (800nm) outputs of the OPO were used simultaneously to irradiate the target. The number of sensing elements used was 90 × 100 with 100 µm element spacing. The total acquisition time was 15 minutes. The maximum intensity projections (MIP) of the reconstructed 3D PA image on the lateral plane (*x*-*y* plane) and one of the vertical planes, *y*-*z* plane are presented in Figure 4(b) and (c), respectively. The lateral MIP clearly reveals the sagittal and transverse sinuses and other cerebral veins. On the vertical MIP, the straight sinus is noticeably visible which extends to a depth of ~2.5 mm.

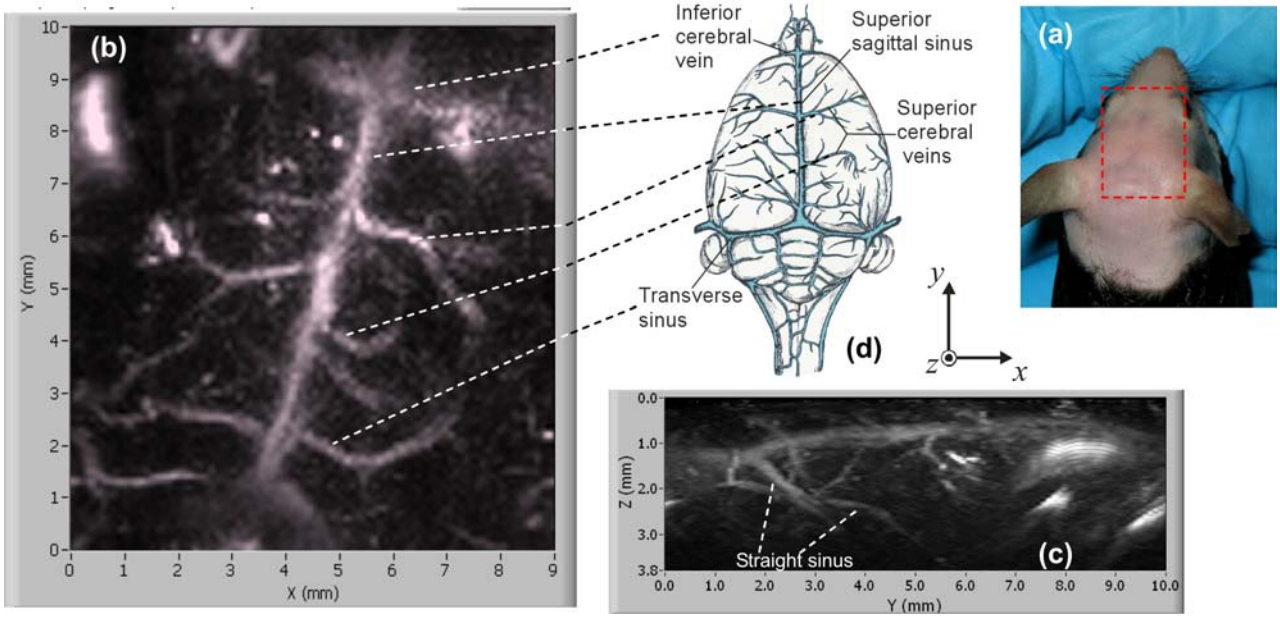

Figure 4: (a) Region over which signals were recorded. The maximum intensity projections (MIP) of the reconstructed 3D photoacoustic image of the mouse brain on (b) the lateral plane (*x*-*y* plane) and, (c) the vertical *y*-*z* plane. (d) A schematic of the anatomy of rodent outer brain circulation system [19]. The reconstructed photoacoustic images can also be viewed as animated volume rendered images at: http://www.medphys.ucl.ac.uk/research/mle/images.htm

4.2. 3D imaging of superficial blood vessels in the skin

Figure 5 shows a photoacoustic image of the skin microvasculature around the abdomen of the mouse. The excitation wavelength was 590 nm. The 3D volume image on the right is reconstructed from the photoacoustic signals mapped over an area of 10 mm × 10 mm with an element spacing of 100 µm. The figure on the upper left hand side is the MIP on the lateral plane. Apart from the superficial microvasculature lying within 0.5 mm depth, large blood vessels at a depth of ~2mm are clearly visible on the 3D volume image as indicated. The MIP image on the lower right hand side is a close-up view within the above imaged area. It was obtained with a finer element spacing 60µm at the same excitation wavelength 590 nm.

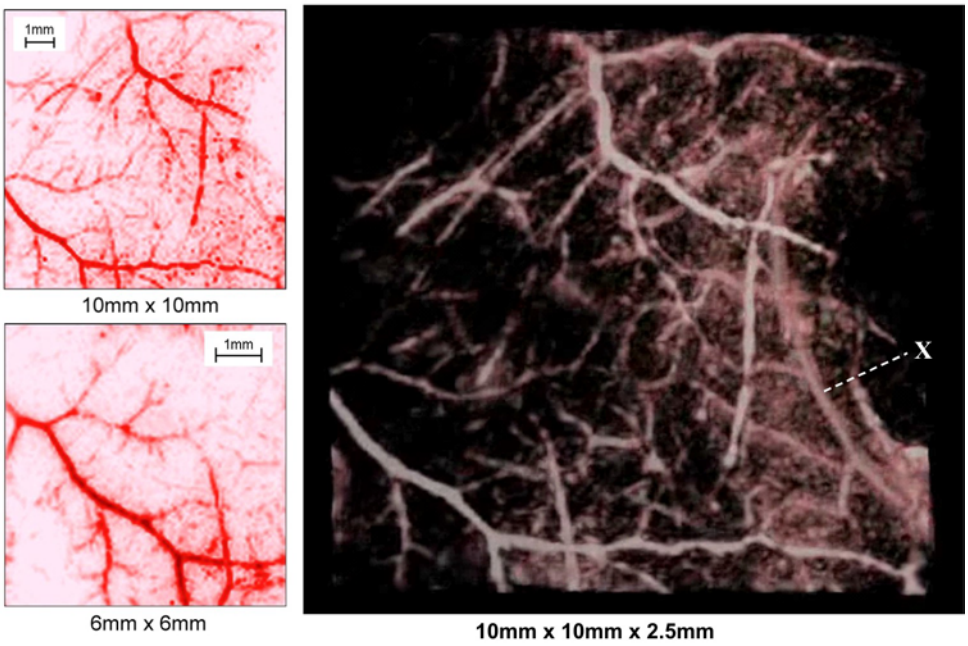

Figure 5: Photoacoustic images on the abdomen area of a mouse with excitation at 590 nm. The vessel marked "X" is located at a depth of 2 mm.

5. CONCLUSION

The capability of a FP ultrasound sensor based 3D photoacoustic imaging system for visualizing vascular structures in soft tissues with high spatial resolution, has been demonstrated. In addition to broadband high acoustic sensitivity, the optical design of the FP sensor also enables the system to perform photoacoustic imaging in backward mode, over a wide excitation wavelength range from 590nm to 1200nm. These features make the system particularly useful for anatomic and functional imaging of the superficial vasculature for the characterising small animal models of cancer and brain injury.

ACKNOWLEDGEMENT

This work is sponsored by the Engineering and Physical Science Research Council, UK.

REFERENCES

1. Andreev VG, Karabutov AA, Solomatin SV, Savateeva EV, Aleynikov V, Zhulina YV, Fleming RD, Oraevsky AA, Optoacoustic tomography of breast cancer with arc-array-transducer, *Proc SPIE* Vol 3916, pp36-47, 2000

2. Kruger R.A., Miller K.D., Reynolds H.E., Kiser Jr W.L., Reinecke D.R. and Kruger G.A., Contrast enhancement of breast cancer in vivo using thermoacoustic CT at 434 MHz, *Radiology*, 216, pp.279-283, 2000

3. Wang X, Pang Y, Ku G, Xie X, Stoica G and Wang L, Noninvasive laser-induced photoacoustic tomography for structural and functional *in vivo* image of the brain, *Nature Biotechnology*, 21 (7), pp.803-806 (2003).

4. Beard PC, Photoacoustic imaging of blood vessel equivalent phantoms, *Proc. SPIE*, Vol. 4618, pp.54-62, 2002.

5. Magdalena C. Pilatou, Nico J. Voogd, Frits F. M. de Mul, Wiendelt Steenbergen, and Leon N. A. van Adrichem, Analysis of three-dimensional photoacoustic imaging of a vascular tree in vitro, *Rev. Sci. Instrum.*, vol.74, pp.4495-4499, 2003.

6. Hoelen CG, de Mul FFM, Pongers R, Dekker A, Three-dimensional photoacoustic imaging of blood vessels in tissue, *Optics Letters*, Vol 23, No 8, pp648-650, 1998

7. Zhang H F, Maslov K, Stoica G and Wand L V, Functional photoacoustic microscopy for high-resolution and noninvasive *in vivo* imaging, *Nature Biotechnology*, Vol 24 (7), pp.848-851, 2007.

8**.** Beard PC and Mills TN., An optical fibre sensor for the detection of laser generated ultrasound in arterial tissues, *Proc* SPIE Vol 2331, pp112-122, 1994

9. Beard PC, Perennes F, Mills TN, Transduction mechanisms of the Fabry Perot polymer film sensing concept for wideband ultrasound detection., *IEEE Transactions on Ultrasonics, Ferroelectrics and Frequency control*, Vol 46, No 6, pp1575-1582, 1999.

10. Zhang EZ and Beard P, Broadband ultrasound field mapping system using a wavelength tuned, optically scanned focused laser beam to address a Fabry Perot polymer film sensor, *IEEE Transactions on Ultrasonics, Ferroelectrics, and Frequency Control*, vol.53, pp.1330-1338, 2006.

11. Lamont M and Beard PC, 2D imaging of ultrasound fields using a CCD array to detect the output of a Fabry Perot polymer film sensor, *Electronics Letters* 42(3), pp.187-189, 2006.

12. Askenazi S, Witte R, O'Donnell M, High frequency ultrasound imaging using a Fabry Perot etalon, *Proc SPIE* Vol 5697, pp243-250, 2005

13. Beard PC**,** Zhang EZ, Cox BT, Transparent Fabry Perot polymer film ultrasound array for backward-mode photoacoustic imaging, *Proc. SPIE* 5320, pp230-237, 2004

14. Laufer J, Elwell CE, Delpy DT, Beard PC, *In vitro* measurements of absolute blood oxygen saturation using pulsed near-infrared photoacoustic spectroscopy: accuracy and resolution, *Physics in Medicine and Biology*, 50, pp 4409–4428, 2005

15. Laufer JG, Delpy DT, Elwell CE, Beard PC, Quantitative spatially resolved measurement of tissue chromophore concentrations using photoacoustic spectroscopy: application to the measurement of blood oxygenation and haemoglobin concentration, *Physics in Medicine and Biology*, 52, pp141168, 2007.

16. Edward Z. Zhang and Paul Beard, 2D backward-mode photoacoustic imaging system for NIR (650-1200nm) spectroscopic biomedical applications, *SPIE Proc*. 6086, pp.60860H1-8, 2006

17. Cox, BT, and Beard, PC, Frequency dependent directivity of a planar Fabry Perot polymer film ultrasound sensor, IEEE Transactions on Ultrasonics, *Ferroelectrics and Frequency control* 54, pp.394-404, 2007.

18. Koestli K, Frenz M, Bebie H, Weber H, Temporal backward projection of optoacoustic pressure transients using Fourier transform methods, *Physics in Medicine and Biology*, **46,** pp1863-1872, 2001

19. Eunice Chace Greene, *Anatomy of the Rat*, Philadelphia : American Philosophical Society, 1935